

Final Report

EECE7244

INTRODUCTION TO MICRO-ELECTROMECHANICAL SYSTEMS

Fall 2023



Project: MEMS Cantilever-Based Radiation Detector

Project F Team Members:

Anand Raj

Cherisma Tanduru

Jobin Geevarghese Thampi

Ray Tong

Suchibrata Das

Submission Date: *December 13, 2023*

Table of Contents

Abstract.....	3
Problem Description	4
Device Performance Specifications	4
Device Design Overview	4
Polystyrene Coating.....	5
Polysilicon Cantilever Beam.....	5
Electrostatic Actuator	5
Piezoresistive Sensor	5
Packaging	5
External Microcontroller.....	6
Governing Equations of the Cantilever Beam	6
Electrostatic Actuation	8
Material Properties and Initial Device Specifications.....	9
Mechanical Sensitivity of the Radiation Sensor	10
Dynamic Simulink Modeling	10
Electrical Sensitivity of the Radiation Sensor	12
Final Device Response to Radiation Exposure	14
Device Fabrication Process	15
Future Work.....	21
References	22

Abstract

This project introduces a MEMS cantilever-based gamma radiation detector, utilizing a polysilicon cantilever coated with polystyrene, sensitive to gamma radiation exposure. The design incorporates an electrostatic actuator and a piezoresistive sensor in a Wheatstone bridge for detecting radiation-induced resonance frequency shifts. Theoretical modeling, device design, and fabrication processes are detailed, highlighting the device's ability to detect low radiation doses, with a targeted sensitivity of 0.13mGy. The project replaces traditional bulky, expensive equipment with a compact, cost-effective solution. Future work includes exploring polystyrene's response to higher radiation doses and enhancing the signal-to-noise ratio, vital for industrial applications. This innovative approach marks a significant step in radiation detection technology, particularly relevant in taking precautions and corrective measures in the expanding nuclear energy sector.

Problem Description

The type of radiation our MEMS sensor will be designed to detect is gamma radiation. Gamma radiation is the most harmful type of radiation because it is invisible and ionizing, and unlike alpha and beta particles, it can penetrate deep into the human body causing molecular damage. Small doses of gamma radiation exposure may not cause immediate health effects but can increase cancer risk by damaging DNA. This makes it important to create effective and inexpensive gamma radiation sensors.

Some applications for a MEMS radiation sensor include radiation dosage monitoring for workers (mining, nuclear industry, healthcare), radiation release sensing for places where radioactive material is stored, and monitoring radiation levels following a nuclear accident.

Global nuclear energy capacity is expected to keep increasing as nations respond to climate change, which will lead to more nuclear energy plants, more nuclear storage sites, and increased uranium mining activity. This creates an expanding market for radiation sensors.

Device Performance Specifications

The unit of measurement for radiation that will be used when discussing device performance is gray (Gy). It is a measure of the absorbed dose of radiation energy deposited in a unit mass of matter (J/kg). The sievert (Sv) is another common unit used for radiation, but for “equivalent dose” rather than “absorbed dose.” The equivalent dose is used to find health effects on the human body. Fortunately for gamma radiation, the conversion between Gy and Sv is 1:1.

To determine performance specifications for a radiation sensing device, it is useful to use radiation’s effect on human health as a reference point. According to the CDC, mild radiation sickness can occur with a short-term exposure of 0.3 Gy, and death is a possibility at 1.2 Gy. [1] On the other end of the scale, there is background gamma radiation from natural sources. In North America, the background radiation from natural sources is 3.1 mGy per year. [2] If a radiation sensor is sensitive enough, the background radiation from natural sources would need to be accounted for when measuring dosages over extended periods of time. One last point of reference is the maximum allowable radiation exposure for workers who work with and around radioactive materials. The U.S. Nuclear Regulatory Commission sets the dose limit for workers to 50 mGy per year. [3]

At this initial stage of the project, the team will target the ability to sense a radiation dose of 0.13mGy. This is the dose limit of 50 mGy divided by 365 days. If this target is not achieved, the radiation sensor would still be useful for detecting either short-term high intensity radiation or long-term low intensity radiation near a radiation source.

Device Design Overview

The MEMS radiation sensor to be designed by the project team will consist of a polysilicon cantilever beam with a polystyrene coating. The resonant frequency of the cantilever beam is expected to change when the sensor is exposed to gamma radiation. The cantilever beam will be actuated by an electrostatic drive and the tip deflection of the beam will be measured using a piezoresistor in a Wheatstone bridge circuit. An external microcontroller will provide the input signal for the electrostatic drive and receive the output of the Wheatstone bridge circuit.

Polystyrene Coating

A thin polystyrene coating will be the primary source of radiation sensitivity for the device. Polystyrene has been shown to undergo physical changes when exposed to low radiation doses. The physical changes were measurable through surface roughness [4] and transmission spectra. [5] Both measurements are linearly correlated with radiation exposure. These physical changes in the polystyrene coating could affect the stiffness and damping provided by the polymer layer. Since the equation for resonant frequency being used does not include damping, the effect of radiation of the stiffness (Young's Modulus) of the polystyrene coating will be focused on. The nominal thickness of the polystyrene will be 0.1 μ m, based on spin coating deposition methods that have been used on silicon substrates before [4] [6].

Polysilicon Cantilever Beam

The cantilever beam is made of polysilicon. The thickness of the beam will be kept low at 1 μ m, to maximize the effect of the polystyrene coating. 500 μ m will be used as a starting value for the length, and 90 μ m will be used as a starting value for the width. These dimensions should guarantee a functional sensor since they are based on a published device with experimental data. [4] The project team will then refine these dimensions as necessary to maximize the device's sensitivity to radiation. A polysilicon cantilever beam alone experiences no resonant frequency shift when exposed to radiation. [7] This allows any resonant frequency shift with radiation exposure to be attributed to the polystyrene coating.

Electrostatic Actuator

The cantilever beam will be electrostatically actuated by an electrode also made of polysilicon. Both the polysilicon in the beam and the electrode will be heavily doped so that they are conductive.

This structure is externally excited using a voltage source. When a voltage is applied across these plates, they become oppositely charged, creating an electrostatic force that attracts the plates. Since the electrode is bonded to the substrate, the flexible cantilever beam will move towards the electrode, resulting in oscillation if the input signal is modulated.

Piezoresistive Sensor

A section of the polysilicon beam near the fixed end is turned into a piezoresistor through polysilicon doping. A Wheatstone bridge is then connected to this piezoresistor on the beam. As the cantilever beam bends, the piezoresistor on the beam will be strained, changing the resistance of the piezoresistor. The Wheatstone bridge translates the change in resistance into an output voltage.

Packaging

We are making use of Thin Film Packaging (also called integrated encapsulation approach) method for this device. In the integrated encapsulation approach the devices are processed first, without etching any sacrificial layers needed for release of the device. Another sacrificial layer is then deposited and patterned atop the device layer. Next, an encapsulation layer is deposited and patterned with a fluid access hole. Finally, after etching of the sacrificial layer, the fluid access holes are sealed under vacuum either using CVD thin films, evaporated metals, or solder. Having the sensor's packaging fully cover the radiation sensing cantilever beam should have a minimal effect on device performance, since gamma radiation can penetrate over 10mm into lead. [8]

External Microcontroller

An external microcontroller will provide the input signal for the electrostatic drive in the form of a sine wave signal with constant voltage amplitude and varying frequency. The microcontroller will then analyze the output of the Wheatstone bridge circuit as a function of tip deflection. The input signal frequency that produces the greatest output amplitude would be identified as the resonant frequency of the beam, allowing the radiation dosage of the beam to be deduced.

Governing Equations of the Cantilever Beam

At this initial stage of the project, we will use simplified values for m_{eff} (effective mass), c (damping coefficient), and k_{eff} (effective spring stiffness). To simplify the analysis, the cantilever beam of the radiation sensor will be modelled with a constant rectangular cross-section, and material properties are assumed to be uniform.

The first natural frequency of most cantilever sensors is given by:

$$f = \frac{1}{2\pi} \left(\frac{1.875}{L} \right)^2 \sqrt{\frac{EI}{\rho A}} \quad (1)$$

where E , I and A are the Young's modulus, moment of inertia, and the cross-sectional area of the beam. [9] The resonant frequency and effective spring constant k_{eff} define the effective mass m_{eff} of the cantilever in the following way:

$$f_0 = \frac{1}{2\pi} \sqrt{\frac{k_{eff}}{m_{eff}}} \quad (2)$$

The effective mass can be found out using the formula:

$$m_{eff} \approx 0.24m_0 \quad (3)$$

Where m_0 is the total mass of the beam (mass of polysilicon and polystyrene combined) and can be calculated using the formula:

$$m_0 = L * w * (t_{Si} * \rho_{Si} + 2t_{PS} * \rho_{PS}) \quad (4)$$

Where L is the length of the cantilever beam, w is the width of the beam, t_{Si} is the thickness of the polysilicon structural layer, t_{PS} is the thickness of each layer of polystyrene coating, and ρ is the densities of the two materials.

The effective spring constant for a cantilever beam is typically calculated using:

$$k_{eff} = \frac{3EI}{L^3} \quad (5)$$

However, since the radiation sensor cantilever beam is made of two materials (polysilicon and polystyrene), the calculation of k_{eff} is more complicated. EI needs to be replaced by $E_{Si}I_{Si} + E_{PS}I_{PS}$, using the Young's Modulus of each material and their individual moments of inertia based on geometry.

$$k_{eff} = \frac{3(E_{Si}I_{Si} + E_{PS}I_{PS})}{L^3} \quad (6)$$

Since their beam remains symmetrical after coating with polystyrene, I_{Si} can be calculated using the standard equation:

$$I_{Si} = \frac{w * t_{Si}^3}{12} \quad (7)$$

I_{PS} of the top and bottom polystyrene layers combined can be calculated using:

$$I_{PS} = \frac{w((t_{Si} + 2t_{PS})^3 - t_{Si}^3)}{12} = \frac{w(3t_{Si}^2t_{PS} + 6t_{Si}t_{PS}^2 + 4t_{PS}^3)}{6} \quad (8)$$

We expect E_{PS} to change with radiation dose, and now need an equation to express that relationship. We propose that the equation for $E_{PS}(r)$ is:

$$E_{PS}(r) = E_{PS0}(1 + \gamma_{PS} * r^2) \quad (9)$$

Where r is the radiation dose measured in Gy and γ_{PS} is the constant relating radiation dose with the change in the Young's modulus of a polystyrene film.

Equation 9 enables us to use the linear association between radiation dose and resonant frequency shift described in reference [4] for modeling purposes, even though it may not accurately reflect the physics involved.

Combining equations 2, 5, 6, and 9, an equation for the resonant frequency shift due to radiation exposure can be derived:

$$\Delta f(r) = \frac{r}{2\pi} \sqrt{\frac{3 * I_{PS} * E_{PS0} * \gamma_{PS}}{m_{eff} * L^3}} = \frac{r}{2\pi} \sqrt{\frac{(3t_{Si}^2t_{PS} + 6t_{Si}t_{PS}^2 + 4t_{PS}^3) * E_{PS0} * \gamma_{PS}}{0.48(t_{Si} * \rho_{Si} + 2t_{PS} * \rho_{PS}) * L^4}} \quad (10)$$

Using equation 10 and the radiation dose-frequency data from Figure 1, we calculated that the radiation constant $\gamma_{PS} = 2.7024 \times 10^7 \text{ Gy}^{-2}$.

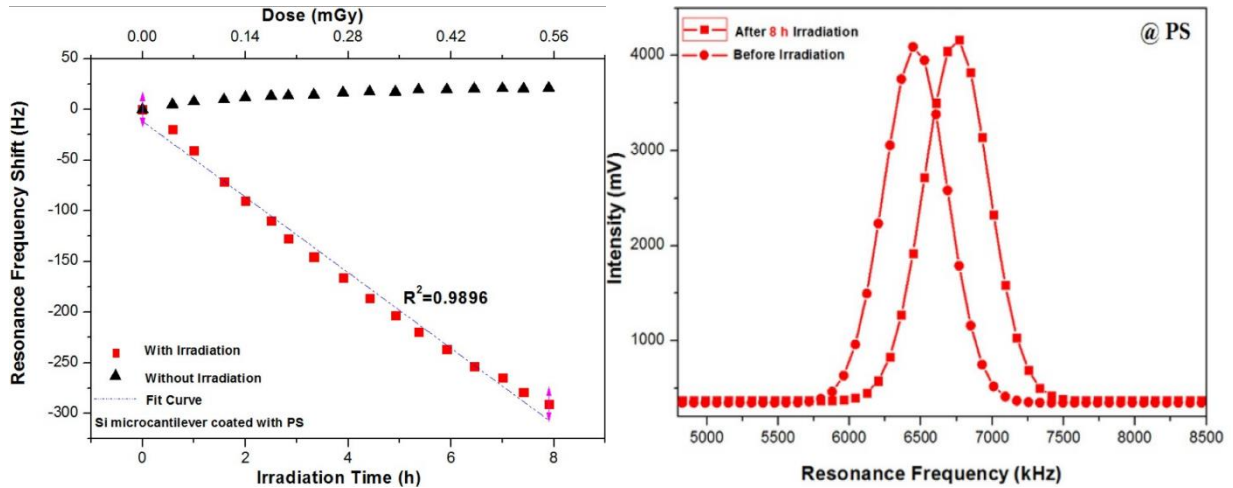


Figure 1 Frequency Response Data from Reference [4]

Lastly, to complete a dynamic model of the cantilever, the damping coefficient b was derived from experimental data. Since we planned to package our device in vacuum, the primary source of damping would be structural damping. The damping ratio of a cantilever beam in vacuum was measured to be $\zeta = 0.82 \times 10^{-4}$ [10]. This damping ratio can then be converted to the damping coefficient:

$$b = 2\zeta \sqrt{m_{eff} * k_{eff}} \quad (11)$$

The damping coefficient will have no effect on the resonant frequency but will determine the amplitude of deflection of the cantilever beam when it is resonating.

Electrostatic Actuation

The relationship between the input voltage, V_{in} and the force applied at the tip of the cantilever beam is described by the following formula:

$$F = \frac{\epsilon w l_o}{2g^2} V_{in}^2 \quad (12)$$

Where ϵ is relative permittivity of air $8.85 \times 10^{-12} Fm^{-1}$ and g is the distance between the cantilever beam tip and electrode.

We now have all the variables necessary to create a representative mass-spring-damper system. [10]

Material Properties and Initial Device Specifications

Table 1 Material Properties and Initial Device Dimensions

Parameter	Value
Length of the Cantilever, L	500 μm
Width of the Cantilever, w	90 μm
Thickness of the polysilicon cantilever, t_{Si}	1 μm
Thickness of polystyrene coating, t_{PS}	0.1 μm
Length of electrode, l_e	100 μm
Initial gap, g_0	2.5 μm
Young's Modulus, E	
I. Polysilicon, E_{Si}	160 GPa
II. Polystyrene, E_{PS}	3.25 GPa
Density, ρ	
I. Polysilicon, ρ_{Si}	2330 Kg/m ³
II. Polystyrene, ρ_{PS}	1070 Kg/m ³

Using these initial device specifications, we can create a plot of the expected resonant frequency of the sensor due to radiation exposure.

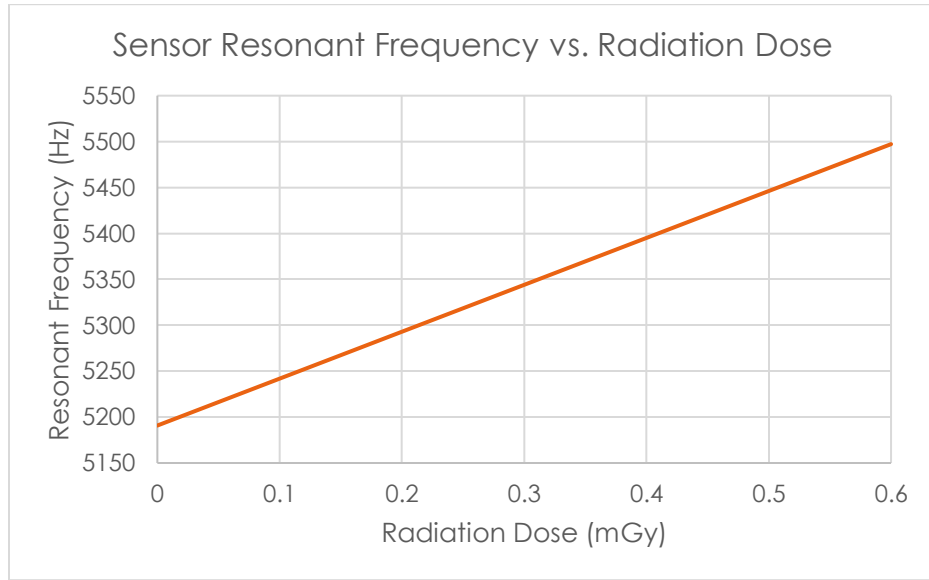


Figure 2 Theoretical Resonant Frequency Response from Radiation Exposure

While the theoretical dimensions were the same, the initial resonant frequency from our calculations is different from the experimental data in Figure 1. This is due to the experimental cantilever beam having imperfect geometry and the Young's modulus of the experimental beam's materials may not be the same value as the ones used in our calculations. This should not be a problem for the sensor design since the initial resonant frequency of each sensor beam can be calibrated for. Only the resonant frequency shift would be needed to measure the radiation dosage.

Mechanical Sensitivity of the Radiation Sensor

Equation 10 can be re-arranged to create a formula for mechanical sensitivity of the device:

$$\frac{\Delta f}{\Delta r} = \frac{1}{2\pi} \sqrt{\frac{(3t_{Si}^2 t_{PS} + 6t_{Si} t_{PS}^2 + 4t_{PS}^3) * E_{PS0} * \gamma_{PS}}{0.48(t_{Si} * \rho_{Si} + 2t_{PS} * \rho_{PS}) * L^4}} \quad (13)$$

Based on the sensitivity formula, device performance can be improved by increasing the polystyrene coating thickness, and by decreasing the length of the beam. Decreasing the length of the beam has the largest effect in theory. Reducing the length would also mean reducing the width to maintain beam behavior as we require a certain amount of width is required to fabricate the piezo resistor. Increasing the polystyrene coating thickness is risky to implement due to the limited experimental information available for the effect of radiation on polystyrene and coating process. Ultimately, we chose to keep the initial device dimensions.

Dynamic Simulink Modeling

A Simulink model was created using the device dimensions, material properties, governing equations of the beam and electrostatic actuation equations. The Simulink model was used to test different input voltages to see what value would provide the right amount of deflection when the beam was resonating. At resonance, the beam deflects far more than what would be predicted by a static model, so the use of Simulink was the simplest way to model this. Figure 3 below is the Simulink model used.

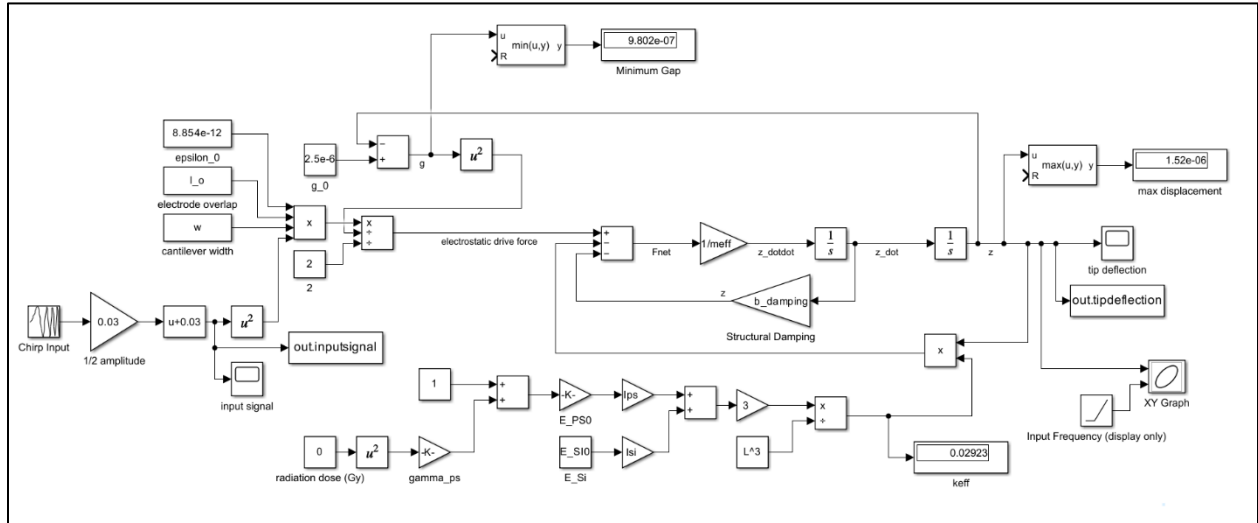


Figure 3 Simulink Model of Electrostatically Actuated Beam

The input signal was configured as a “Chirp” signal, where the amplitude remains constant, but the frequency increases with time. This inputted signal effectively sweeps through frequencies over time to guarantee that the input frequency will match the resonant frequency of the beam at some moment, resulting in increased beam tip displacement.

A trial and error approach was used to find an input voltage that would result in the most possible tip displacement without reaching zero gap at resonance. The optimal input signal we chose was a biased

sine wave of 60mV amplitude and variable frequency, shown in Figure 4, which resulted in a maximum tip deflection of 1.52 μm , shown in Figure 5.

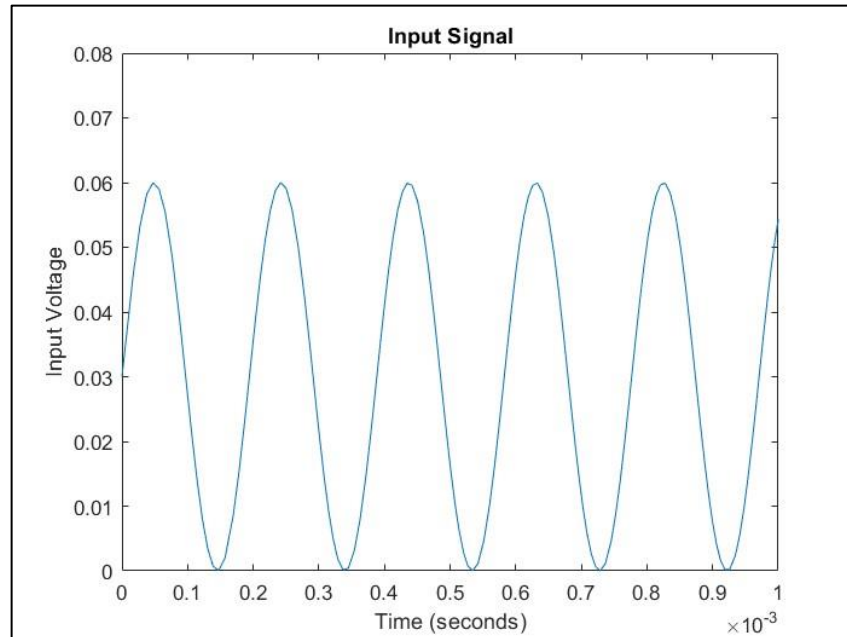


Figure 4 Input Signal at Approximately 5000Hz

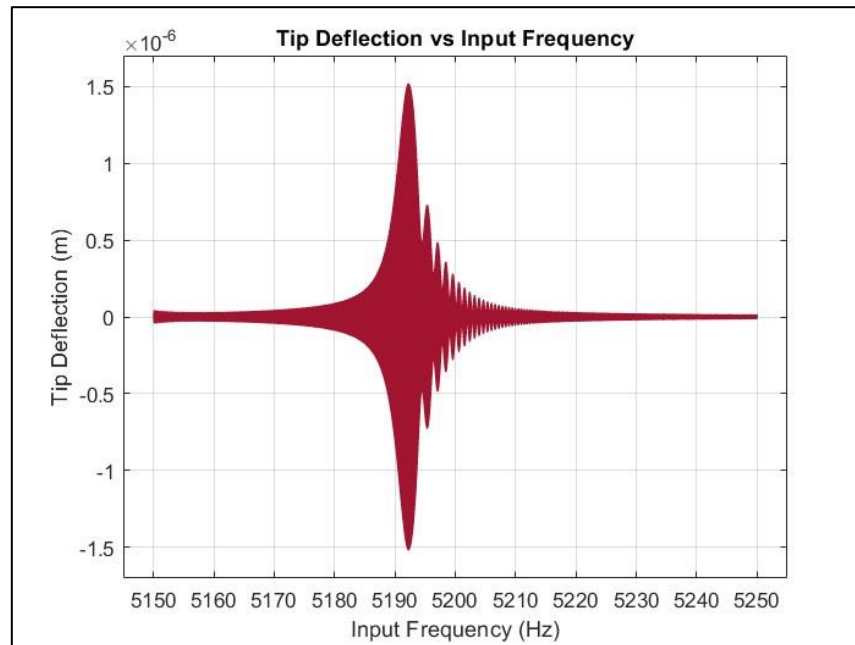


Figure 5 Tip Deflection from 60mV Input Voltage, Frequency swept 5150Hz to 5250Hz over 10 seconds

The Simulink model also demonstrated that our system was sufficiently underdamped to create a large difference between tip deflection at resonant frequency versus tip deflection at a random frequency. Figure 5 demonstrated a tip deflection at resonance over 30 times greater in magnitude than tip deflection when the input frequency was not near the resonant frequency.

Electrical Sensitivity of the Radiation Sensor

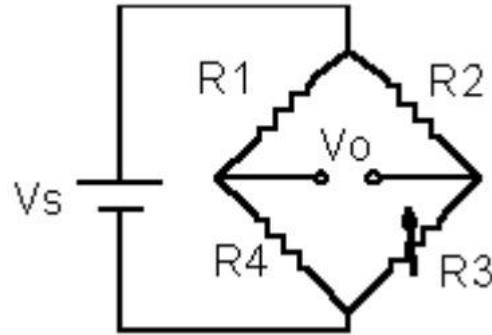


Figure 6 Example Wheatstone Bridge Circuit

The beam tip deflection will be measured using a piezoresistor on the beam. As the beam bends, the resistance of the piezoresistor will change, and this change in resistance can be measured using a Wheatstone bridge. One of the Wheatstone bridge's resistors will be the piezoresistor on the beam. In this case we are considering R3 to be piezoresistor on the cantilever beam. The Wheatstone bridge translates this change in resistance into a voltage output, V_{out} .

With R3 acting as a variable resistor, V_{out} can be calculated using:

$$V_{out} = \left[\frac{R3}{R2 + R3} - \frac{R4}{R4 + R1} \right] V_{bridge} \quad (14)$$

When R3 changes to $(R3 + \Delta R)$ and $\Delta R \ll R3$, so we get:

$$V_{out} = \left[\frac{R1\Delta R}{(R2 + R3)(R1 + R4)} \right] V_{bridge} \quad (15)$$

In case of a balanced $\frac{1}{4}$ active Wheatstone bridge for small outputs [11],

$$\frac{V_{out}}{V_{bridge}} \approx \frac{\Delta R}{4R} \quad (16)$$

From [11] we can conclude that the voltage force sensitivity is given by

$$S_{FV} = \frac{3(L - 0.5l_p)\pi_l}{2wt_{Si}^2} \gamma V_{bridge} \beta^* \quad (17)$$

Where $\pi_l = 72 \times 10^{-11} Pa^{-1}$ is the piezoresistive coefficient of polysilicon [11] and l_p is the length of the piezoresistor. We assume β^* (efficiency factor) to be unity. γ is the geometry factor which is assumed to be 0.70 [11]. From S_{FV} and the effective spring constant equation (6), we get the voltage displacement sensitivity as:

$$S_{dv} = \frac{3E_{si}t_{si}(L - 0.5l_p)\pi_l V_{bridge}}{8L^3} \quad (18)$$

Since $S_{dv} = \frac{V_{out}}{z}$, we get:

$$V_{out} = z \left\{ \frac{3E_{si}t_{si}(L - 0.5l_p)\pi_l V_{bridge}}{8L^3} \right\} \quad (19)$$

Figure 7 below shows the output signal of the Wheatstone bridge with $V_{bridge} = 12V$, using the tip deflection data from Figure 5.

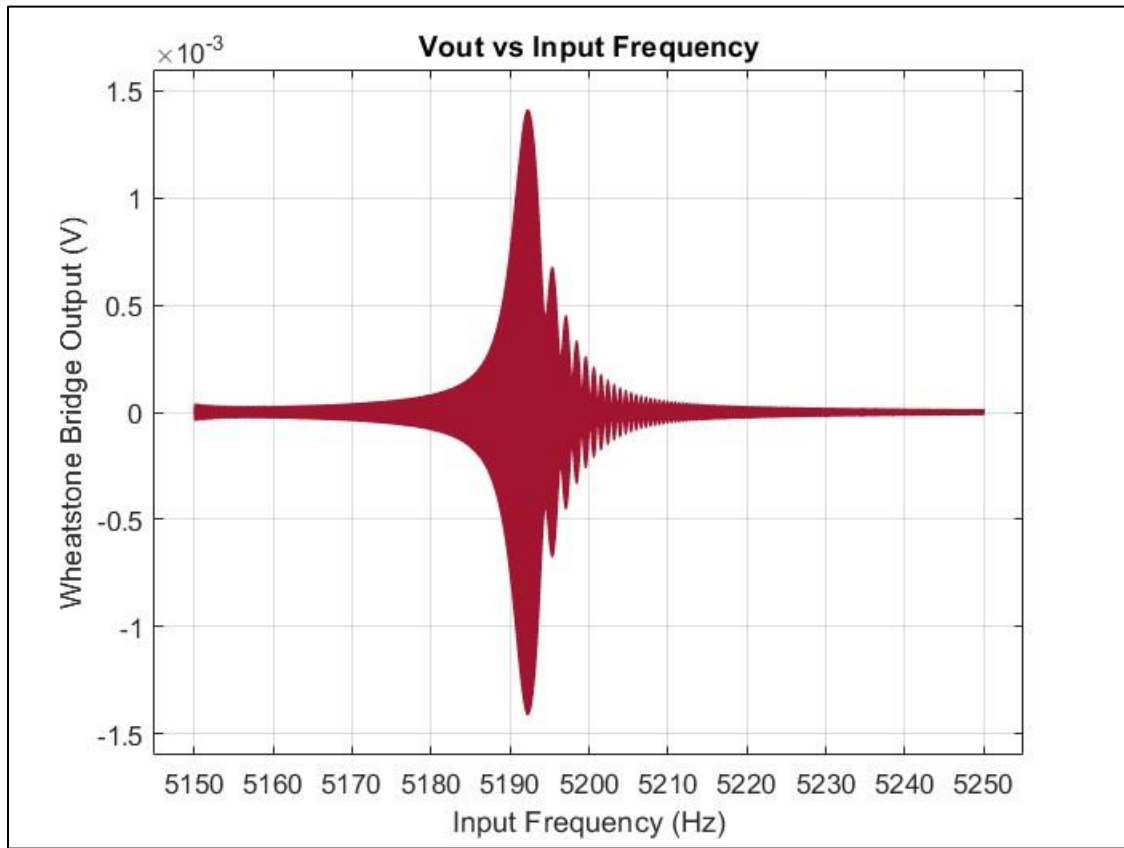


Figure 7 Wheatstone Bridge Output, Frequency swept 5150Hz to 5250Hz over 10 seconds

With this output from the Wheatstone bridge, a microcontroller can analyze the signal and identify what input frequency corresponded with the highest amplitude voltage output, therefore identifying the resonant frequency of the cantilever beam at the time.

Final Device Response to Radiation Exposure

The final Simulink model is shown below in Figure 8.

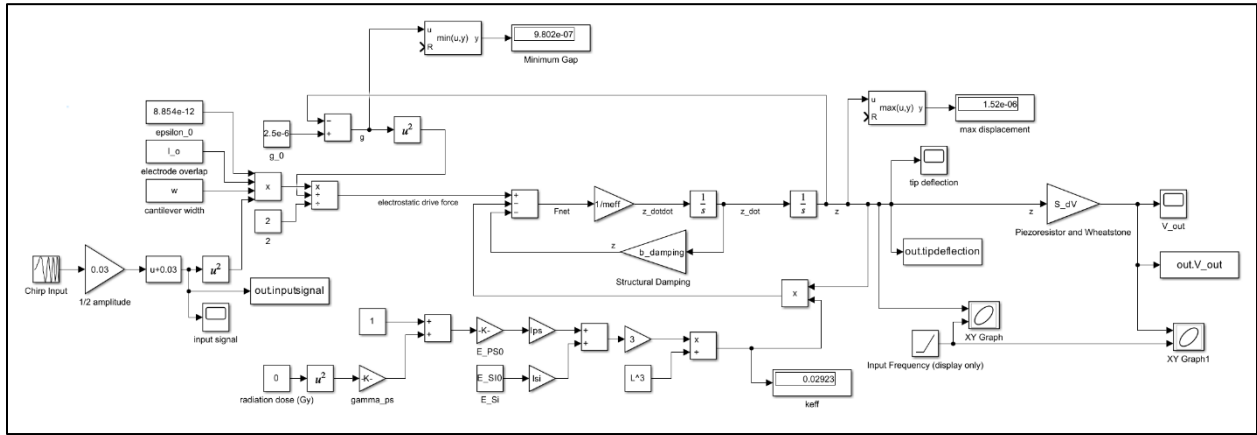


Figure 8 Final Simulink Model with Wheatstone Bridge Output

Since we want to demonstrate the response of the system to radiation exposure, the frequency sweep was expanded to 5150Hz – 5550Hz over 40 seconds. Increasing the input frequency at a rate of 10Hz per second seemed to be slow enough to allow resonance behavior to fully develop despite the frequency never staying constant. Reducing the rate of frequency change had little effect on the peaks observed in the figures below.

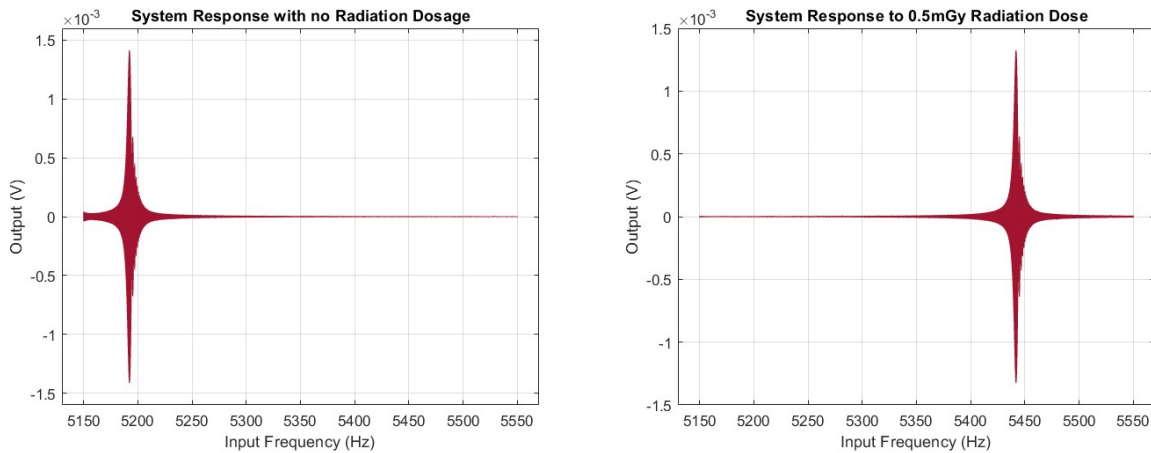


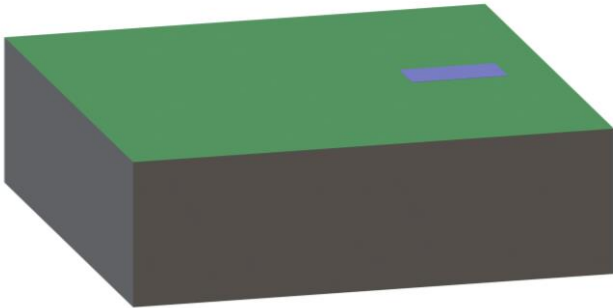


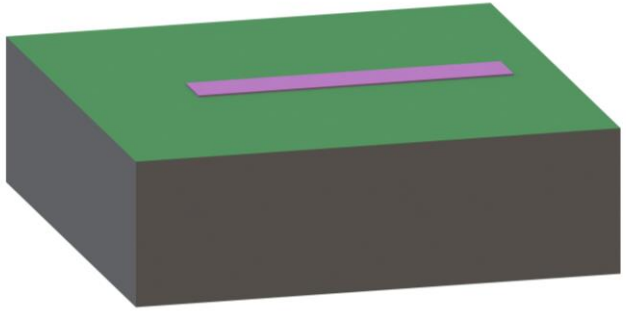
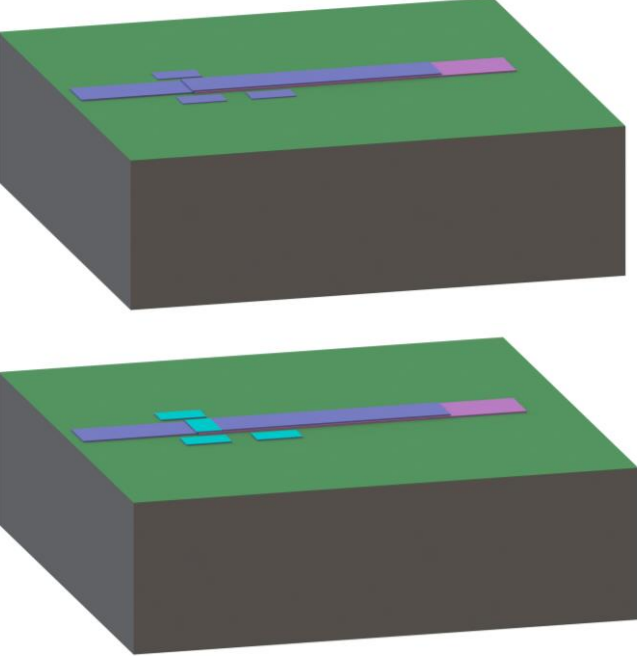
Figure 9 System Response, no radiation on left, 0.5mGy radiation dose on right

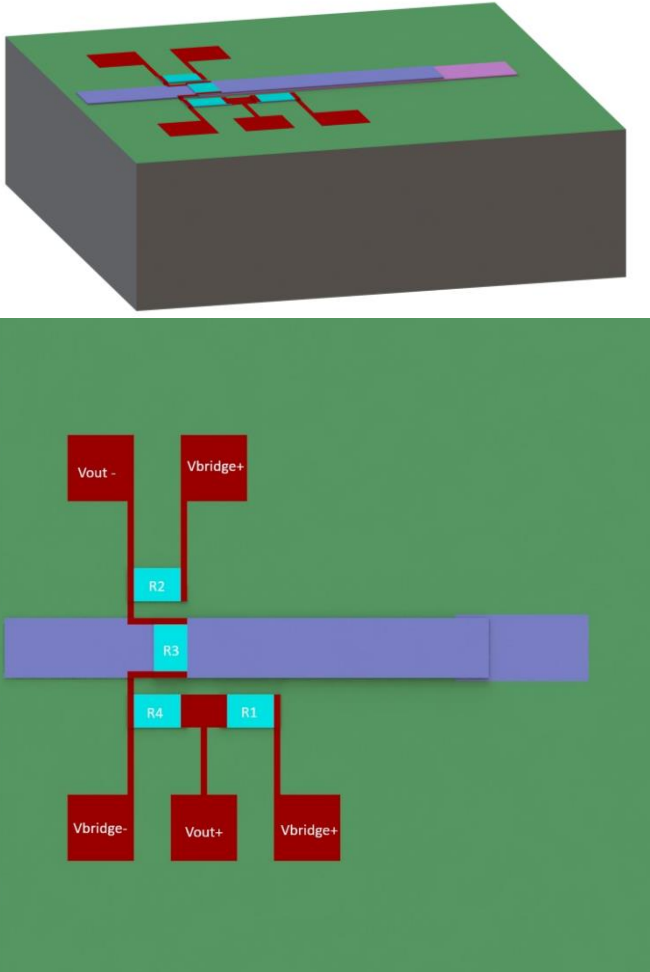
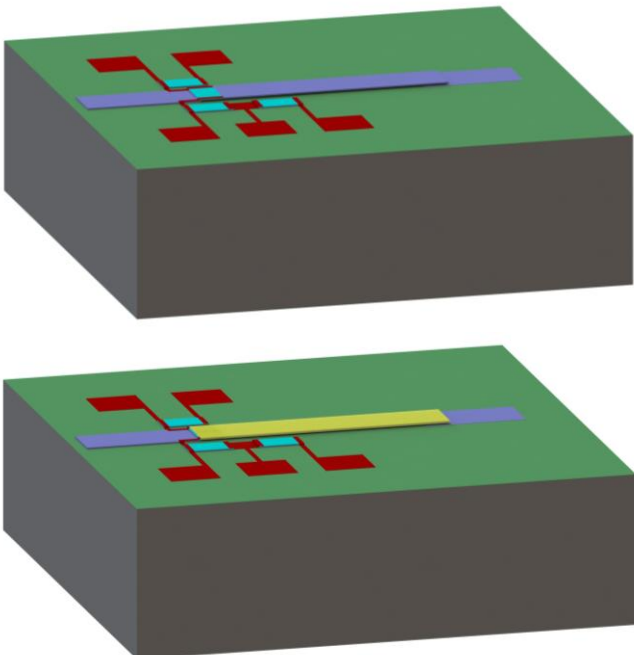
The resonant frequency shift demonstrated by the Simulink model is extremely close to the theoretical values in Figure 2. A resonant frequency of 5446Hz was predicted for a 0.5mGy dose. The Simulink system response peaks at 5442Hz with the 0.5mGy dose.

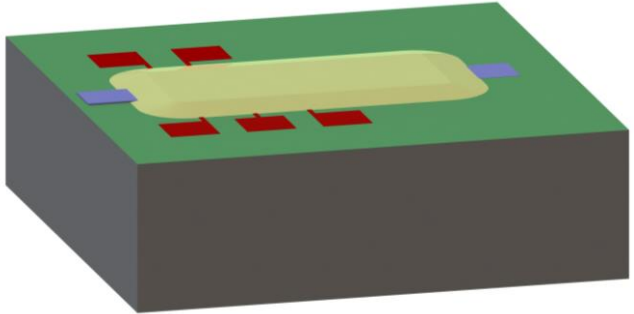
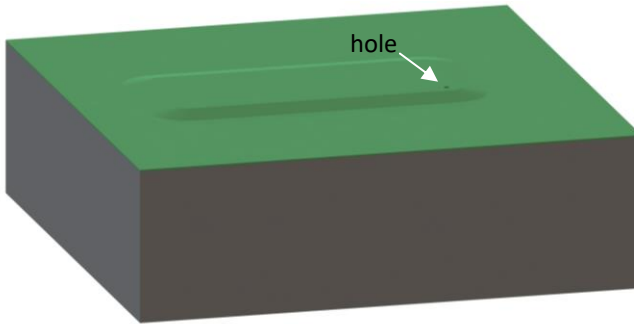
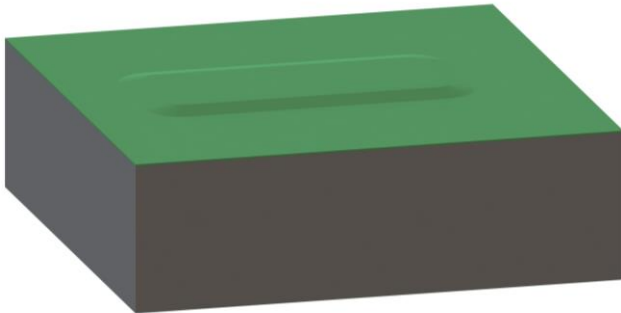
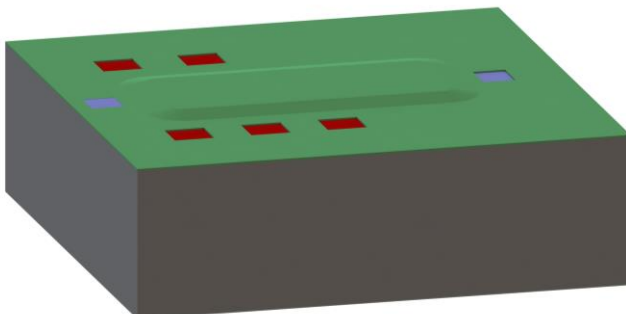
In the actual device, the frequency sweep range would need to be larger to detect higher radiation doses than 0.5mGy. A larger range of frequencies would take longer to sweep through, but a measurement of radiation doses every few minutes is still reasonable for a device intended to measure radiation levels over days or months.

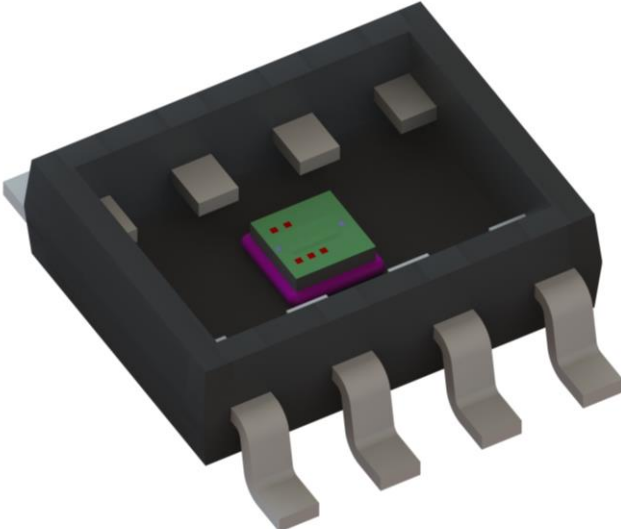
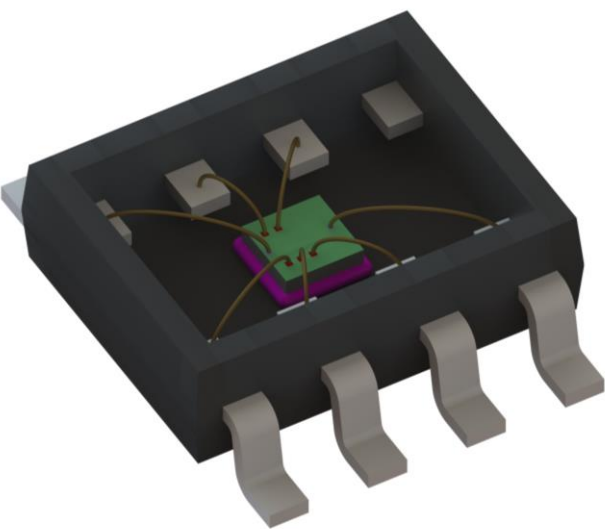
Device Fabrication Process

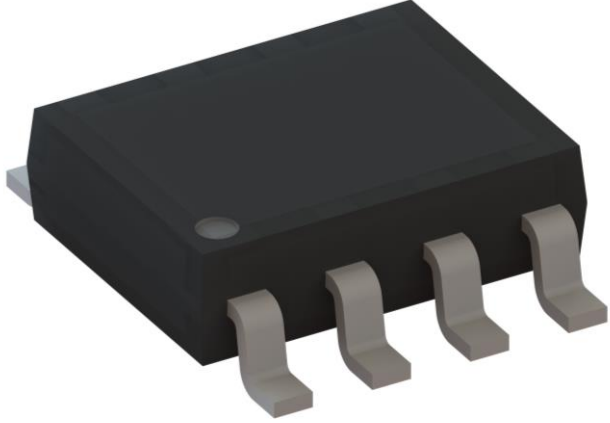

Step	Process Description	Figure
1.	Start with a silicon wafer which is 300um thick. For reference, the die size will be 1mm x 1mm.	 A 3D perspective view of a rectangular silicon wafer. The top surface is a light gray color, and the side surfaces are a darker gray. The wafer is shown from an isometric perspective, highlighting its thickness and rectangular shape.
2.	Clean the wafer using Piranha followed by RCA Method to remove any contaminants.	
3.	Deposit 0.2um of Silicon nitride by LPCVD Method. This layer will function as an insulator.	 A 3D perspective view of a rectangular silicon wafer. The top surface is now a solid green color, representing the deposited silicon nitride layer. The side surfaces remain the same dark gray color as the original wafer.
4.	Deposit 1um of Polysilicon using LPCVD Method. Deposit 0.5um of Positive Photoresist (PR) by spin coating method. Perform photolithography to define the electrode using the mask shown in the adjacent figure and then perform RIE dry etching to remove the polysilicon.	 A 3D perspective view of a rectangular silicon wafer. The top surface is green, representing the polysilicon layer. A small, rectangular blue feature is visible on the top surface, representing the photoresist mask used for etching.
5.	Remove the Photoresist using Acetone and clean the wafer by piranha method and RCA Process	

6.	<p>LPCVD 0.5um of silicon dioxide, shown in pink. This will be a sacrificial layer. Deposit 0.5um Photoresist. The mask to perform the next photolithography step is shown in the adjacent figure. Use RIE dry etching to etch away the silicon dioxide which is not covered by the mask.</p>	
7.	<p>Remove the Photoresist using Acetone and clean the wafer by piranha method and RCA Process (Skip Step 2.)</p>	
8.	<p>Deposit 1um of Polysilicon on top of SiO₂ by LPCVD process, shown in blue. Next, introduce the dopant BPSG (Borophosphosilicate Glass) into the Polysilicon at the fixed end to make it piezoresistive. BPSG deposition is carried out through Chemical Vapor Deposition (CVD) followed by annealing. This annealing process activates the dopants, allowing them to effectively diffuse into the PolySi layer. Uniform distribution of doping is crucial during annealing to achieve the desired electrical properties in the piezoresistor. This process is carried out to make four resistors shown in cyan. 3 positioned on the wafer and one on the cantilever beam. The 4 resistors will have identical dimensions and therefore the same initial resistance.</p>	

9.	<p>After the formation of these 4 piezo resistors, connections are made between them to form a Wheatstone bridge. The connections are made of gold, shown in red, which is deposited using sputter deposition and a mask.</p>	 <p>The top diagram is a 3D perspective view of a cantilever beam on a substrate. It shows a central purple piezoresistive strip with four red rectangular piezoresistors (R1, R2, R3, R4) deposited on its surface. Red gold lines connect these resistors to form a Wheatstone bridge circuit. The bottom diagram is a 2D top-down view of the same cantilever. It labels the resistors as R1, R2, R3, and R4. The electrical connections are labeled: Vout- and Vbridge+ at the top left; Vbridge- and Vout+ at the bottom left; and Vbridge+ at the bottom right. The central purple strip is labeled R3.</p>
10.	<p>Once the Cantilever is released, we will dry using super-critical CO₂ drying. Cantilever is then immersed for one hour in a solution of solvent and dissolved polystyrene.</p>	 <p>The top diagram is a 3D perspective view of the cantilever after release, showing the central purple strip and the four red piezoresistors. The bottom diagram is a 3D perspective view of the cantilever after being coated with a yellow layer of polystyrene solution, which is now covering the central purple strip and the red piezoresistors.</p>

11.	Remove the PR using Acetone followed by cleaning the whole device using 49% HF.	
12.	Thin film encapsulation - For encapsulation of the cantilever Deposit PSG layer on the cantilever using LPCVD.	
13.	Using LPCVD deposit a layer of SiN on top of the PSG. This will be the encapsulation layer. SiN layer is patterned with a fluid access hole.	
14.	Isotropically etch PSG Layer with 49% HF	
15.	Another layer SiN is deposited under vacuum, sealing the fluid access hole. This process encapsulates the cantilever beam in a vacuum environment to minimize damping.	
16.	Deposit 0.5um Photoresist. Mask everywhere except for the contact pads of the electrodes and Wheatstone bridge and perform photolithography. Use RIE dry etching to etch away the SiN to expose the contact pads of the electrodes and Wheatstone bridge.	
17.	Remove the Photoresist using Acetone and clean the wafer by	

	piranha method and RCA Process (Skip Step 2.)	
18.	Cut device dies from wafer using a dicing saw	
19.	The whole MEMS device is plastic packaged into the SOIC-8 package size. The device is adhered to plastic using adhesive on the back of the structure, shown in pink.	
20.	Final integration - The MEMS die is wire bonded to the pins of the packaging. The plastic packaging can then be closed. The complete package can be soldered onto a circuit board to connect to a microcontroller (not shown).	

		
21.	<p>The device is to be tested at this stage to verify the function of the electrostatic actuation, piezoresistive sensing, and that the initial resonant frequency of the beam is as expected. Testing cannot be done earlier in the process since a microprocessor is needed to provide the input signal and analyze the output of each individual device.</p>	 <p>1: Vbridge- 5: Vinput-</p> <p>2: Vout+ 6: Vout-</p> <p>3: Vbridge+ 7: Vbridge+</p> <p>4: Vinput+ 8: NC</p>

Conclusion

The project team successfully advanced the concept demonstrated by [4]. While the amount of frequency shift from radiation exposure could not be improved due to the lack of experimental data, the final device designed by the team outlines a possible path to creating a commercially viable radiation sensor. The bulky and expensive laser used to measure the resonance frequency was replaced by an on-die piezoresistive sensing system and a relatively inexpensive microcontroller. A reasonable packaging solution was also designed to protect the radiation sensing cantilever beam from the environment. Lastly, even though the radiation sensitivity of the device was not improved, the device appears sensitive enough to meet our original target of detecting a 0.13mGy radiation dose.

Future Work

To advance the development of the project device further, more experimental data is required. Areas that would benefit from additional experimental data include the effect of changing the polystyrene coating thickness and the effect of higher radiation doses on polystyrene. While the relationship between gamma radiation exposure and the material properties of polystyrene appeared linear at doses below 1mGy, that may not hold true for higher doses.

Signal noise is another aspect of the design that has not been analyzed due to time constraints. The amplitude of the output signal of our current Wheatstone bridge was near 1mV, which is at a very high risk of being lost in noise. Since the radiation detector will be deployed in industrial environments, there would likely be sources of electromagnetic interference from nearby electrical equipment. Improving the performance of the piezoresistive sensing by choosing a piezoresistive material with a better piezoresistive coefficient would likely be the first step towards improving the signal to noise ratio. Our output signal amplitude could also be improved by increasing the gap, and therefore allowing more beam deflection. This would also require major changes to the fabrication process, possibly by using KOH on an SOI wafer.

Changes in ambient temperature are an expected source of error that has not been characterized. Polymers are especially susceptible to stiffness changes due to temperature. The team expects that the cantilever-based radiation sensor would need to be deployed alongside a temperature sensor to compensate for the effect of ambient temperature on the resonant frequency of the beam.

References

- [1] CDC, "Acute Radiation Syndrome: A Fact Sheet for Clinicians," CDC, 4 April 2018. [Online]. Available: <https://www.cdc.gov/nceh/radiation/emergencies/arsphysicianfactsheet.htm>. [Accessed 23 October 2023].
- [2] J. Thurston, "NCRP Report No. 160: Ionizing Radiation Exposure of the Population of the United States," *Physics in Medicine & Biology*, vol. 55, no. 20, p. 6327, 2010.
- [3] U.S. NRC, "Information for Radiation Workers," U.S. NRC, 14 December 2021. [Online]. Available: <https://www.nrc.gov/about-nrc/radiation/health-effects/info.html>. [Accessed 23 October 2023].
- [4] K. Shamma, H. Albrithen, B. AlOtaibi and A. Alodhayb, "Ultrasensitive detection of low-dose gamma radiation using polymeric thin films on microelectromechanical system-based sensors," *Journal of Nuclear Science and Technology*, vol. 59, no. 12, pp. 1567-1575, 2022.
- [5] E. C. Onyiriuka, L. S. Hersh and W. Hertl, "Surface Modification of Polystyrene by Gamma-Radiation," *Applied Spectroscopy*, vol. 44, no. 5, pp. 808-811, 1990.
- [6] E. H. Lock and S. G. Walton, "Preparation of Ultra Thin Polystyrene, Polypropylene and Polyethylene Films on Si Substrate Using Spin Coating Technology," United States Naval Research Laboratory, Washington, DC, 2008.
- [7] B. Stark, J. Berstein and R. Lawton, "The Effects of Radiation on the Resonant Frequency of a Polysilicon Microstructure," in *Micro-Electro-Mechanical Systems Reliability & Qualification*, Pasadena, 1998.
- [8] Harvard Natural Sciences Lecture Demonstrations, " α , β , γ Penetration and Shielding," [Online]. Available: <https://sciencedemonstrations.fas.harvard.edu/presentations/%CE%B1-%CE%B2-%CE%B3-penetration-and-shielding>. [Accessed 21 November 2023].
- [9] J. X. Zhang and K. Hoshino, "Chapter 6 - Mechanical Transducers: Cantilevers, Acoustic Wave Sensors, and Thermal Sensors," in *Molecular Sensors and Nanodevices*, William Andrew Publishing, 2014, pp. 321-414.
- [10] H. Sumali and T. G. Carne, "Air Damping on Micro-Cantilever Beams," Sandia National Lab, Albuquerque, NM, 2007.
- [11] S.-J. Park, J. C. Doll, J. A. Rastegar and B. L. Oruitt, "Piezoresistive Cantilever Performance—Part II: Optimization," *Journal of Microelectromechanical Systems*, vol. 19, no. 1, pp. 149-161, 2009.
- [12] C. Shin, I. Jeon, Z. G. Khim, J. W. Hong and H. Nam, "Study of sensitivity and noise in the piezoelectric self-sensing and self-actuating cantilever with an integrated Wheatstone bridge circuit," *Review of Scientific Instruments*, vol. 81, no. 3, 2010.
- [13] J. S. Mitchell, "LOW TEMPERATURE WAFER LEVEL VACUUM PACKAGING USING AU-Si," University of Michigan, Michigan, 2008.